STABILITY IN AN EVAPORATING CHAIN OF IDENTICAL DROPLETS

A. F. Ginevskii, A. S. Dmitriev,
and D. A. Ovechkin

UDC 533.6.0111

Stability has been examined for an ordered chain of monodisperse droplets under vacuum, which interact one with another via the evaporating molecules.

There are many processes based on ordered flows of monodisperse materials, where an important aspect is to maintain the order [1]. The original structure may be disrupted because of a spread in the initial velocities [2] or because of external factors such as electric and magnetic fields or interaction with a low-density gas. If the particles are charged, Coulomb forces can disrupt the system. However, even uncharged droplets can interact because of evaporation and condensation. Here we examine how such processes influence the stability.

We consider droplets at temperature T in an infinite chain moving with velocity v. In a coordinate system moving with velocity v, the chain is at rest in the initial state. In the spaces between the drops, there is a vapor produced by evaporation, which expands in accordance with the ratio of the distance a between adjacent drops to the mean free path λ. One can estimate λ from [3] $\lambda \sim (\pi d^2 n_S)^{-1}$ (Table 1). The saturation vapor pressures of the substances were taken from [2, 4]. If $\lambda \gg a$, one can neglect collisions between molecules in the space around the drops, in which case the interactions are calculated as follows.

The rate of evaporation j from unit surface is defined by the Hertz-Knudsen formula [5]:

$$j = \varkappa n_s (k_B T / 2\pi m_0)^{1/2}. \quad (1)$$

The evaporation (condensation) coefficient κ for simplicity is taken as one. If $r \ll L$, a droplet can be considered as a point source of rectilinearly moving molecules. Then the force F between droplets due to the momentum transferred by the molecules is

$$F = 2k_B T n_s r^4 / L^2 = \gamma / L^2. \quad (2)$$

That force is thus analogous to a Coulomb repulsion force in that approximation. In this model, the first particle (source) is considered as a point source of molecules, which is applicable not only for $r \ll L$. If this is violated, (2) gives an upper bound to F.

The potential energy U of a chain composed of N drops can be derived in the harmonic approximation on the assumption that only nearest neighbors interact:

TABLE 1. Mean Free Paths for Molecules of Various Substances

Substance	Temperature, K	Saturation vapor pressure, Pa	Mean free path, μm
Lithium	453,7	$1{,}19 \cdot 10^{-8}$	$1 \cdot 10^{12}$
	700	$3{,}56 \cdot 10^{-2}$	$5 \cdot 10^{5}$
	1000	97,2	300
Sodium	450	$1{,}63 \cdot 10^{-5}$	$2 \cdot 10^{7}$
	500	$9{,}49 \cdot 10^{-2}$	$1{,}5 \cdot 10^{5}$
	700	109	180
DC-200 oil	301	$7{,}6 \cdot 10^{-7}$	$3 \cdot 10^{8}$

Moscow Power Institute. Translated from Inzhenerno-fizicheskii Zhurnal, Vol. 60, No. 4, pp. 656-660, April, 1991. Original article submitted July 31, 1990.

0022-0841/91/6004-0501$12.50

$$U = -\frac{\gamma}{2a^3}\sum_{\alpha,n} f_\alpha (x_{n,\alpha} - x_{n-1,\alpha})^2, \tag{3}$$

in which

$$f_\alpha = \begin{cases} 1 & \text{if} \quad \alpha = 1, 2, \\ 2 & \text{if} \quad \alpha = 3. \end{cases} \tag{4}$$

If M is the mass of a drop, the kinetic energy of the entire system is

$$K = \frac{M}{2}\sum_{\alpha,n} \dot{x}^2_{n,\alpha}. \tag{5}$$

We seek the solution as a superposition of quasicontinuous waves [6]:

$$x_{n,\alpha} = \sum_{\alpha,k} A_{k,\alpha} \exp(ikna), \tag{6}$$

in which k is the set of all nonequivalent values of the wave numbers, $k = 2\pi\nu/N\cdot a$; $\nu = 0, \pm 1, \pm 2, \ldots, N/2$.

The equations of motion are solved for the new variables $A_{k\alpha}$, and the transformation [6] to (6) then gives that: for $\alpha = 1, 2$

$$x_{m,\alpha}(t) = \frac{1}{N}\sum_{k,n}\left[x_{n,\alpha}(0)\operatorname{ch}(\Omega_k t) + \frac{\dot{x}_{n,\alpha}(0)}{\Omega_k}\operatorname{sh}(\Omega_k t)\right]\exp[i(m-n)ka], \tag{7}$$

and for $\alpha = 3$

$$x_{m,\alpha}(t) = \frac{1}{N}\sum_{k,n}\left[x_{n,\alpha}(0)\cos(\sqrt{2}\Omega_k t) + \frac{\dot{x}_{n,\alpha}(0)}{\sqrt{2}\Omega_k}\sin(\sqrt{2}\Omega_k t)\right]\times\exp[i(m-n)ka], \tag{8}$$

in which Ω_k is the frequency of mode k, which is

$$\Omega_k \equiv \Omega(k) = \Omega(-k) = 2(\gamma/Ma^3)^{1/2}|\sin(ka/2)|. \tag{9}$$

We see from (8) that the droplet motion along the axis is oscillatory; (7) implies that a droplet is also unstable in a position perpendicular to the axis. The maximal instability increment from (9) is

$$\Omega_{\max} = 2(\gamma/Ma^3)^{1/2} = (6k_B T n_S r/\pi a^3)^{1/2}. \tag{10}$$

The reciprocal of Ω_{max} defines the characteristic instability growth time:

$$\tau \sim (a^3/n_S T r)^{1/2}. \tag{11}$$

As $n_S(T)$ is exponential, we conclude that the instability is governed mainly by the temperature.

Estimates may be made. For drops of oil (Table 1) at 301 K, with r = 100 μm and a = 1000 μm, the characteristic instability time is τ = 72 sec. Figure 1 fives calculated τ(T) for liquid metals. For lithium at a given temperature, the increment is less than for sodium, since the first has a lower vapor pressure.

The transverse instability for a flow of evaporiting droplets increases the velocity variance and also the deviations from the equilibrium position. The over-all variance will be determined by the initial value (which is entirely dependent on the production device) and by this instability. We established the contribution from the latter to the velocity variance and the deviations.

Let the displacements of all the droplets from the equilibrium positions be zero at the start: $x_{n,\alpha}(0) = 0$. Then (7) gives the velocity of droplet m in the transverse direction (subscript α omitted) as

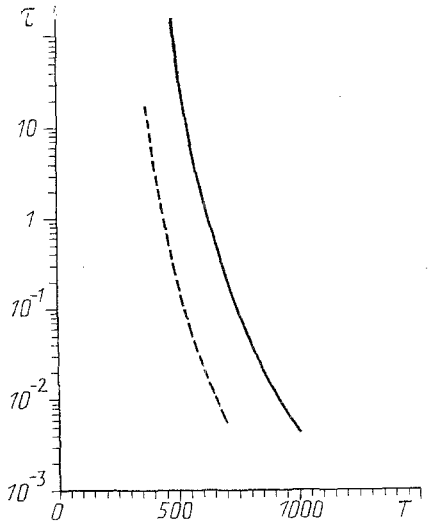

Fig. 1

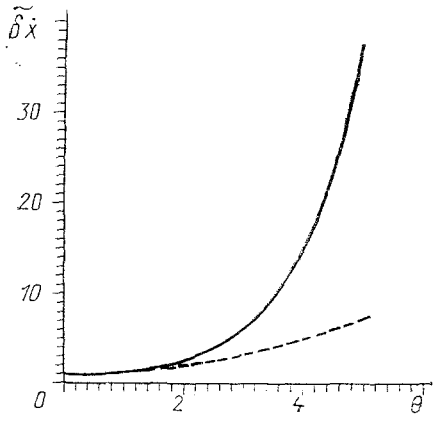

Fig. 2

Fig. 1. Characteristic instability time for a chain of liquid metal droplets as a function of temperature (droplet radius 100 μm, distance apart 100 μm). Solid line lithium, dashed line sodium. τ in sec, and T in K.

Fig. 2. Dimensionless standard deviation for the velocity of an individual droplet as a function of dimensionless time. Solid line from (14), dashed line from (15).

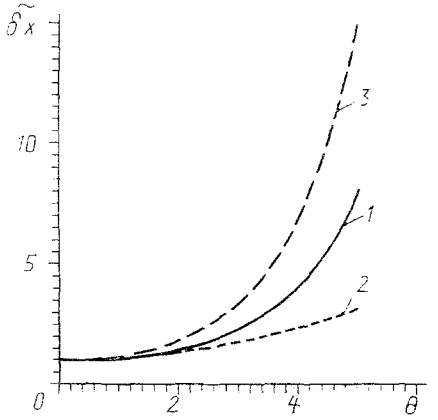

Fig. 3. Dimensionless standard deviation from the equilibrium position as a function of dimensionless time: 1) from (16); 2) from (17); 3) (18) estimate.

$$\dot{x}_m(t) = \frac{1}{N}\sum_{k,n}\dot{x}_n(0)\,\mathrm{ch}\,(\Omega_k t)\exp[i(m-n)ka]. \tag{12}$$

The interval between adjacent k tends to zero for $N \to \infty$, so one can replace $\sum_k \ldots$ by $(N\cdot a/2\pi)\int_{-\pi/a}^{\pi/a}\ldots dk$. Integration [7] gives

$$\dot{x}_m(t) = \sum_n (-1)^{m-n}\dot{x}_n(0)\,I_{2(m-n)}(\Omega_{\max}t), \tag{13}$$

in which $I_{2(m-n)}$ is Bessel function of the first kind and imaginary argument with order 2(m-n). We introduce the dimensionless time $\theta = t/\tau = \Omega_{\max}t$ and assume that the droplet

velocities are not correlated at the start, while the velocity distribution has standard deviation $\delta\dot{x}(0)$ (the same for each droplet), to get the dimensionless standard deviation of the velocity as a function of time as

$$\tilde{\delta}\dot{x} \equiv \frac{\delta\dot{x}(\theta)}{\delta\dot{x}(0)} = \sqrt{I_0^2(\theta) + 2\sum_{S=1}^{N/2} I_{2S}^2(\theta)}. \tag{14}$$

Up to quantities of the second order of smallness relative to θ we have

$$\tilde{\delta}\dot{x}(\theta) = 1 + \frac{1}{4}\theta^2. \tag{15}$$

Figure 2 shows (14) and (15). As in the derivation of (14), we get a formula for the dimensionless standard deviation of the displacement from the equilibrium position. It is convenient first to integrate (12) with respect to time, and then

$$\tilde{\delta}x(\theta) \equiv \frac{\delta x(\theta)}{\delta x_0(\theta)} = \frac{1}{\theta}\sqrt{\left\{\int_0^\theta I_0(\xi)\,d\xi\right\}^2 + 2\sum_{S=1}^{N/2}\left\{\int_0^\theta I_{2S}(\xi)\,d\xi\right\}^2}, \tag{16}$$

in which $\delta x_0(\theta) = \delta\dot{x}(0)\theta/\Omega_{max}$ is the deviation for noninteracting droplets. For $\theta \ll 1$, (16) becomes

$$\tilde{\delta}x(\theta) = 1 + \frac{1}{12}\theta^2. \tag{17}$$

It is of interest to derive $\tilde{\delta}x(\theta)$ in another way. We note that (7) has the upper bound $(\dot{x}_{n,\alpha}(0)/\Omega_{max})\,\mathrm{sh}\,(\Omega_{max}t)$, so the deviation in dimensionless form does not exceed

$$\tilde{\delta}x(\theta) = \mathrm{sh}\,\theta/\theta. \tag{18}$$

The dimensionless standard deviations in the transverse coordinate are given by (16)-(18) and are shown in Fig. 3.

Even relatively slight evaporation (molecular state) can lead to instability in a monodisperse flow. The characteristic instability growth time is governed primarily by the temperature but is also dependent on the flow geometry. The transverse instability contributes to the velocity and displacement variances, with the variations occurring more slowly than exponentially.

These trends should be considered in devising any system involving a flow of monodisperse material [8].

NOTATION

a, distance between equilibrium positions of two adjacent droplets (lattice constant); $d = 3\cdot10^{-10}$ m, gas-kinetic molecular diameter; F, force between two droplets; j, evaporating-molecule flux density; K, kinetic energy; k, wave number, k_B, Boltzmann's constant; L, distance between drops; $M = 4\pi\rho r^3/3$, drop mass; m_0, molecular mass; $N(N\to\infty)$, number of droplets in a chain; $n_S = n_S(T)$, equilibrium molecular concentration in vapor; r, drop radius; t, time; U, potential energy; v, droplet chain speed; $x_{n,\alpha} = x_{n,\alpha}(t)$; α, coordinate of droplet with number n; $\dot{x}_{n,\alpha} = \dot{x}_{n,\alpha}(t)$, projection of velocity on the α direction; λ, molecular mean free path; κ, evaporation (condensation) coefficient; $\gamma = 2k_BTn_S(T)r^4$, coefficient of proportionality in the formula defining force as a function of distance between drops; $\Omega_k = \Omega(k)$, instability increment; Ω_{max}, maximum value for instability increment; ρ, density; τ, characersitic instability time; θ, dimensionless time; δx, $\tilde{\delta}x$, dimensional and dimensionless standard deviations of droplet position from equilibrium position; δx_0, standard deviation for a droplet not interacting with others; and $\delta\dot{x}$, $\tilde{\delta}\dot{x}$, dimensional and dimensionless standard deviations in droplet from equilibrium position

LITERATURE CITED

1. A. F. Ginevskii and A. S. Dmitriev, Coll. from Moscow Power Institute [in Russian], No. 149 (1987), pp. 5-24.
2. M. Dixon, AIAA Pap. No. 77 (1985), pp. 1-12.
3. E. M. Lifshits and L. P. Pitaevskii, Physical Kinetics [in Russian], Moscow (1979).
4. P. L. Kirillov, Yu. S. Yur'ev, and V. P. Bobkov, Handbook on Thermohydraulic Calculations: Nuclear Reactors, Heat Exchangers, and Steam Generators [in Russian], Moscow (1984).
5. O. Knake and I. N. Stranskii, Usp. Fiz. Nauk, No. 2, 261-305 (1959).
6. A. S. Davydov, Solid-State Theory [in Russian], Moscow (1976).
7. A. P. Prudnikov, Yu. A. Brychkov, and O. I. Marichev, Integrals, Series, and Elementary Functions [in Russian], Moscow (1981).
8. E. P. Muntz and M. Dixon, AIAA Pap. No. 305 (1985), pp. 1-15.

THE BOUNDARY LAYER ON A REGULAR DROPLET CHAIN IN CONTROLLED MOTION

V. I. Bezrukov, A. S. Vasil'ev,
N. A. Razumovskii, and E. F. Sukhodolov

UDC 532.5:66.069.83

The retardation of a droplet chain by air resistance has been examined. Lee's method gives nomograms for the boundary-layer thickness, velocity distribution near the chain, and chain retardation. Experiments show that the model is applicable to important cases.

Regular droplet chains may be used in directing the droplets to one, two, or three traps as well as in recording analog, graphic, and half-tone data and in printing parts of characters.

The viscous friction in air results in momentum transfer from the environment and boundary layers, while the chain itself is retarded. The boundary layer affects the following: the distances between nozzles in multijet printing; the sizes and positions of the traps and of the charging and deflecting electrodes; the lower edges to the characters; the correcting signals, etc. All droplets, no matter what their paths, travel various initial distances in the boundary layers. Figure 1 shows a physical model for determining the main boundary-layer features. Lee's method [1] has been modified for these conditions and gives a mathematical model for the boundary layer. We write the momentum conservation for the mass flows through the current cross section and through the end of the nozzle in the one-dimensional jet representation:

$$\rho_g 2\pi \int_0^{\delta(z)} [a(z)+y]\, v_g^2(z,\ y)\, dy + \rho_\ell \pi a^2(z)\, v_\ell^2(z) = \rho_\ell \pi a_0^2 v_\ell^2. \tag{1}$$

The rate of momentum loss along the path due to boundary-layer friction is

$$-\frac{d}{dz}\left[\rho_\ell \pi a^2(z)\, v_\ell^2(z)\right] = 2\pi a(z)\, \nu_g \left.\frac{\partial v_g(z,\ y)}{\partial y}\right|_{y=0}. \tag{2}$$

The condition for jet continuity is

$$\pi a^2(z)\, v_\ell(z) = \pi a_0^2 v_{\ell 0}. \tag{3}$$

The velocity profile for the air flow in the boundary layer in logarithmic approximation is

Electrojet Technology Center, Leningrad Fine Mechanics and Optics Institute. Translated from Inzhenerno-fizicheskii Zhurnal, Vol. 60, No. 4, pp. 661-668, April, 1991. Original article submitted October 24, 1990.

0022-0841/91/6004-0505$12.50